ELSEVIER

Catalysis Today 56 (2000) 35–44

CATALYSIS TODAY

www.elsevier.com/locate/cattod

# Oxidation of isobutane over supported noble metal catalysts in a palladium membrane reactor

Troy M. Raybold, Marylin C. Huff *

*Center for Catalytic Science and Technology, Department of Chemical Engineering, University of Delaware, Newark, DE 19716, USA*

**Abstract**

Pd membranes are often used to remove the $H_2$ produced in dehydrogenation reactions, thereby relieving the equilibrium limitations on the product yield. These processes, however, can still be limited by the slow kinetics of the dehydrogenation reaction. If $O_2$ is added to the system, the reaction proceeds through both the very fast oxidative dehydrogenation route as well as the dehydrogenation route. Thus, the addition of $O_2$ can suppress a kinetic limitation, while the removal of $H_2$ through the Pd membrane can alleviate the equilibrium limitation imposed on the system by the dehydrogenation route. In this study, we have examined the oxidative dehydrogenation of isobutane in a Pd membrane reactor over Pt/α-$Al_2O_3$ and Rh/α-$Al_2O_3$ monoliths and Pt/γ-$Al_2O_3$ pellets. We have examined $iC_4H_{10}:O_2$ ratios of 1.0 to 2.0, resulting in operating temperatures ranging from 400 to 700°C. While most of this heat is generated by the exothermicity of the reaction, some additional heating was used to boost conversions. Typical contact times ranged from 0.04 to 0.25 s. By continuously removing the $H_2$ produced, isobutylene yields increased. Yield improvements depended strongly on the balance of reaction time with $H_2$ removal time and the importance of the dehydrogenation in the overall reaction scheme. 

*Keywords:* Palladium membrane; Membrane reactor; Oxidative dehydrogenation

## 1. Introduction

The US government passed several amendments to the Clean Air Act in November 1990 in an effort to curb automotive air pollution. The amendments require that gasoline be reformulated to contain at least 2.7% oxygen by weight, while the fraction of high-octane aromatics is limited to 25% by volume [1]. In response to these requirements, methyl *tert*-butyl ether (MTBE) has emerged as a promising, high-octane, oxygen-rich gasoline additive [2]. Since isobutylene is a precursor of MTBE, demand for isobutylene has increased beyond its traditional supply, and the development of additional, efficient methods of producing isobutylene has become necessary.

The typical method of producing isobutylene industrially from isobutane involves dehydrogenation over a $Cr_2O_3/Al_2O_3$ catalyst at ∼650°C [3].

$$iC_4H_{10} \rightleftharpoons iC_4H_8 + H_2 \quad \Delta H_r^0 = +118\,\text{kJ/mol} \quad (1)$$

A large heat input is required to drive this endothermic reaction and maintain the reaction temperature. In addition, carbon deposition can quickly deactivate the catalyst [4,5]. Under typical partially deactivated operating conditions, isobutylene yields are ∼20% [6]. Industrial processes overcome catalyst deactivation by alternating reaction steps and complex regeneration steps. With these novel process designs, isobutylene yields approaching 50% have been reported [7,8].

* Corresponding author. Tel.: +1-302-831-6327; fax: +1-302-831-2085.
*E-mail address:* huff@che.udel.edu (M.C. Huff).

0920-5861/00/$ – see front matter 
PII: S0920-5861(99)00260-6

However, the attainable yield of isobutylene is still limited by thermodynamic equilibrium.

Therefore researchers have proposed conducting dehydrogenation reactions in $H_2$-selective membrane reactors, where the removal of co-produced $H_2$ alleviates the thermodynamic limitation and increases product yield [3,9–24]. In such processes, $H_2$ is selectively removed through a membrane (often Pd or Pd alloy), resulting in an equilibrium shift of the dehydrogenation reaction toward products. Improvements of 50 to 400% in isobutylene yield have been achieved by using a membrane reactor [3,18]. However, many of these membrane reactors operate under a kinetic limitation, since the dehydrogenation reaction is inherently slow [25].

A route to isobutylene which may alleviate this kinetic limitation is the oxidative dehydrogenation of isobutane.

$$i\mathrm{C_4H_{10}} + \tfrac{1}{2}\mathrm{O_2} \rightarrow i\mathrm{C_4H_8} + \mathrm{H_2O}$$
$$\Delta H_r^0 = -124\,\mathrm{kJ/mol} \qquad (2)$$

In contrast to the previous reaction system, Eq. (1), oxidative dehydrogenation is an exothermic reaction with very fast kinetics. Higher yields of isobutylene can be obtained over a $Pt/Al_2O_3$ catalyst at shorter contact times and with much less heat input [26,27]. Fig. 1 shows a schematic of the primary reactions in the oxidative dehydrogenation of isobutane. In these experiments, $O_2$ is the limiting reactant and is usually consumed very quickly after initial contact with the catalyst. Therefore, while oxidative reactions (such as oxidative dehydrogenation, partial oxidation to syngas, and combustion to $CO_2$ and $H_2O$) dominate initially, non-oxidative reactions (such as dehydrogenation and cracking) become increasingly important once $O_2$ is depleted. Note that, in Fig. 1, isobutylene is generated by both, the oxidative and non-oxidative dehydrogenation routes. The dehydrogenation route (in the absence of $O_2$) is thermodynamically limited, and this limitation is affected by the co-production of isobutylene and $H_2$ via oxidative routes.

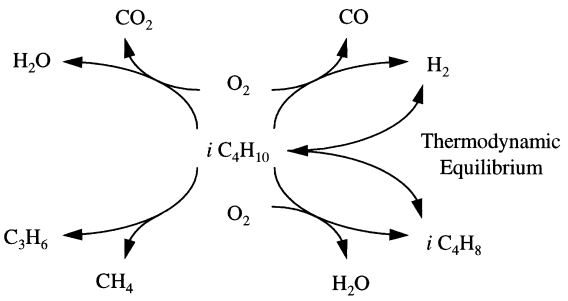


Fig. 1. Schematic of the oxidative dehydrogenation of isobutane reaction system.

In Fig. 2, we show equilibrium values of isobutane conversion and isobutylene selectivity at various $i\mathrm{C_4H_{10}} : \mathrm{O_2}$ ratios and isothermal operating temperatures. Although not shown, $O_2$ conversion is complete under all conditions. For all calculations, there is 10% $N_2$ in the feed. The data in Fig. 2 were obtained by using the HYSYS simulation package to determine the set of products which minimizes the overall Gibbs' free energy at a given feed composition and operating temperature [28]. The allowable products

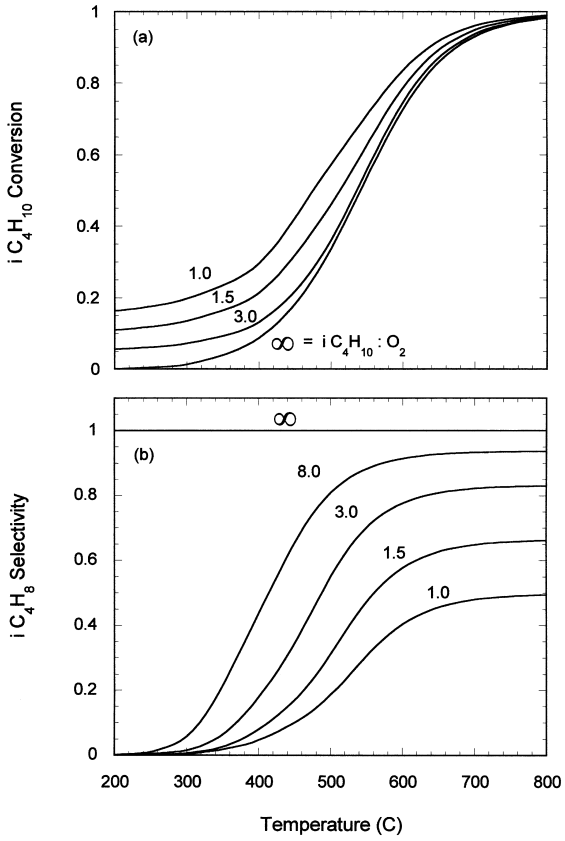


Fig. 2. Calculated (a) equilibrium isobutane conversion, and (b) isobutylene selectivity as a function of temperature and $i\mathrm{C_4H_{10}} : \mathrm{O_2}$ ratio at 10% $N_2$ dilution.

were limited to $i$C$_4$H$_8$, CO, CO$_2$, H$_2$, and H$_2$O. In the low-temperature limit of Fig. 2, deep oxidation of $i$C$_4$H$_{10}$ to CO$_2$ and H$_2$O dominates, so that the isobutylene selectivity and the isobutane conversion are very low. The isobutane conversion is low because the O$_2$ supply is quickly depleted in forming CO$_2$ and H$_2$O. As the temperature increases, dehydrogenation becomes increasingly important, and partial oxidation to CO and H$_2$ becomes more favorable than deep oxidation. In the high-temperature limit, both partial oxidation and dehydrogenation compete, while deep oxidation is not significant. In this limit, the relative importance of partial oxidation and dehydrogenation depends on the amount of O$_2$ fed. When little O$_2$ is available (high $i$C$_4$H$_{10}$ : O$_2$ ratios), dehydrogenation dominates, isobutane conversion is lower, and selectivity to isobutylene is higher; when more O$_2$ is fed (low $i$C$_4$H$_{10}$ : O$_2$ ratios), partial oxidation becomes dominant, conversion increases slightly, and isobutylene selectivity suffers. Although conversion does increase at these lower $i$C$_4$H$_{10}$ : O$_2$ ratios and higher temperatures, Fig. 2 clearly shows that isobutane conversion is still equilibrium-limited. Since O$_2$ is always completely consumed, the data also imply that the equilibrium limitation on the system is imposed by the dehydrogenation reaction. If this limitation can be relieved, the overall isobutylene yield will increase.

Our goal, then, is to combine the advantages of oxidative dehydrogenation (fast kinetics) and dehydrogenation in a membrane reactor (relief of the thermodynamic limitation) by using a Pd membrane reactor in an oxidative dehydrogenation reaction system. We show that isobutylene yield is indeed improved by the removal of H$_2$ through a Pd membrane. The extent of isobutylene yield improvement depends primarily on the balance between catalyst contact time and the characteristic time for H$_2$ diffusion across the membrane. However, the relative importance of the dehydrogenation route in the overall reaction scheme is also an important issue.

## 2. Experimental

### 2.1. Membrane reactor configuration

The oxidative dehydrogenation of isobutane is carried out over both the supported-Pt and supported-Rh catalysts in a stainless-steel flow reactor with a Pd-foil membrane for H$_2$ removal, as illustrated in Fig. 3. The reactor is separated into an upper reaction side and a lower sweep side by the Pd membrane, which is sealed by compression between two copper gaskets. The reactor is 1.6 cm in diameter and each chamber is 7.6 cm in depth. Reactants are premixed, enter the reaction side near the axis, contact the catalyst and membrane, and react to form products which exit through an axial tube. Hydrogen also exits the reaction side by diffusing across the Pd membrane to the sweep side. On the sweep side, N$_2$ enters axially, sweeps away the permeating H$_2$, and then exits. The reactor is externally heated and the entire module is insulated. Temperature is measured by two type K (Chromel/Alumel) thermocouples located on the Pd-foil surface on the sweep side and at the top of the catalyst bed on the reaction side. Both the thermocouples are placed 0.5 cm from the centerline.

### 2.2. Membrane

Two thicknesses (25 and 75 μm) of 99.9% Pd foil were obtained from Alfa Aesar and used as membranes in these experiments, each with an area of 2.0 cm$^2$. Pure Pd was chosen over the more permeable Pd/Ag alloy, since it was more readily available and had a lower fabrication cost. A H$_2$-permeability study of the fresh 75-μm membrane was conducted in an empty reactor over a range of temperatures (150–450°C), and the results are presented in Fig. 4. As expected, the permeability coefficient ($P_m$) could be described by the Arrhenius expression, since permeation through Pd is an activated process:

$$P_m = P_{mo}\left[\exp\left(-\frac{E_p}{RT}\right)\right] \quad (3)$$

In addition, the obtained activation energy ($E_p = 18.6$ kJ/mol) and preexponential factor ($P_{mo} = 0.353$ mol/m/h/atm$^{0.5}$) of the permeability coefficient compare favorably with previously determined values [29–33]. For example, Itoh, et al. [19] measured an $E_p$ of 18.5 kJ/mol and a $P_{mo}$ of 0.370 mol/m/h/atm$^{0.5}$.

### 2.3. Reaction conditions

The feed to the reaction side is $i$C$_4$H$_{10}$ (Matheson, 99.5%), O$_2$ (BOC 99.6%), and N$_2$ (BOC, 99.99%)

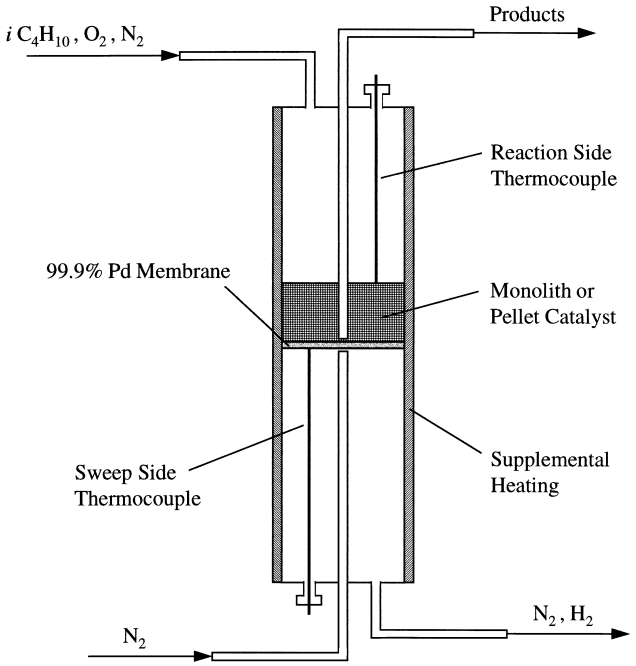


Fig. 3. Sketch of the Pd membrane reactor used in this investigation.

diluent. In all experiments, the diluent is 10% of the total flow. The feed to the sweep side is $N_2$ (BOC, 99.998%). The flow rates of all these species are controlled by Brooks 5850E mass flow controllers. Precise control of the reactants is essential to ensure that the reactor is always operated outside the flammability region. Fig. 5 shows the experimental operating conditions and the flammability region for $i C_4H_{10}$ in a mixture of $N_2$ and $O_2$. We examine $i C_4H_{10} : O_2$ ratios between $1.00 \pm 0.05$ and $2.00 \pm 0.10$ at total reaction side flow rates of $0.30 \pm 0.02$ and $0.85 \pm 0.02$ SLPM. The reactions occur at 400–700°C, resulting in temperature adjusted catalyst contact times ranging from 0.04 to 0.25 s. The sweep side flow rate is maintained at four times the total flow rate to the reaction side. The total pressure on the reaction side is 1.5 psig, while the total pressure on the sweep side is 0.5 psig.

### 2.4. Catalyst

Three catalysts are considered in this study: (1) 0.45 wt.% Pt on an 80 ppi (pores per linear inch) ceramic foam monolith, (2) 0.45 wt.% Rh on an 80 ppi ceramic foam monolith, and (3) a bed of 3.2 mm, 0.5 wt.% Pt/$\gamma$-$Al_2O_3$ eggshell-coated pellets. The monoliths are composed of 92% $\alpha$-$Al_2O_3$ and 8% $SiO_2$. Pt and Rh are deposited separately on the two monoliths by wet impregnation of the support with either a saturated aqueous solution of $H_2PtCl_6$ or a saturated solution of $[Rh(CO_2CH_3)_2]_2$ in acetone,

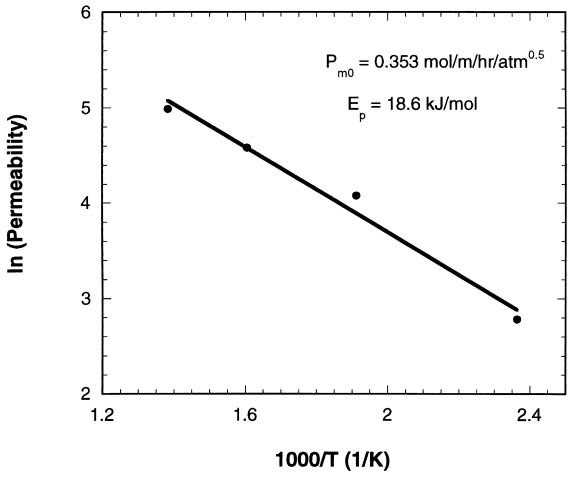


Fig. 4. Temperature effect on permeability coefficient ($10^4$ mol/m/h/atm$^{0.5}$) for the fresh, 75 μm, 99.9% Pd membrane.

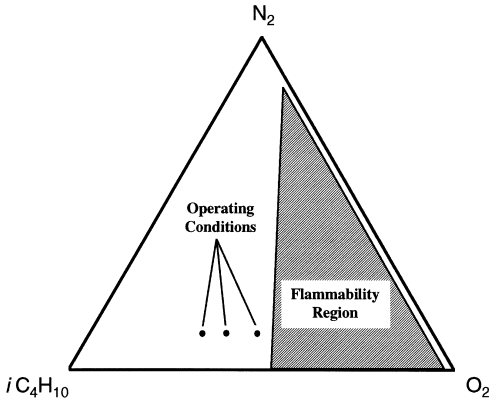


Fig. 5. Flammability region for $i$C$_4$H$_{10}$-O$_2$-N$_2$ mixtures, with experimental operating compositions shown.

followed by calcination in air and reduction in $H_2$. The pellet catalyst is supplied by Alfa Aesar. The reactor side is either loaded with one monolith weighing 1.45 g, with a $N_2$ BET surface area of 0.2 m$^2$/g, or 4.0 g of the pellet catalyst, which has a surface area of 89 m$^2$/g [34].

### 2.5. Product analysis

The effluent compositions from both the reaction side and the sweep side are determined using an on-line HP 6890 gas chromatograph equipped with both flame ionization (FID) and thermal conductivity (TCD) detectors. The measurement of $CH_4$ concentration in both the FID and TCD, and the measurement of the inert $N_2$ concentration in the TCD serve as internal standards. The concentrations of all components except $H_2O$ are measured relative to calibration standards. The concentration of $H_2O$ is determined by an oxygen atom balance. The remaining atom balances (carbon and hydrogen) close to within 10%. For all the results presented below, selectivities ($S_i$) for carbon-containing species are calculated on a carbon atom basis:

$$S_i = \frac{c_i y_i}{\sum_j c_j y_j} \times 100 \quad (4)$$

where $c_i$ is the number of carbon atoms in species $i$, and $y_i$ represents the moles of species $i$. The summation is carried out over all the species. Selectivities for $H_2$ and $H_2O$ are calculated similarly on a hydrogen atom basis.

### 2.6. Typical operation

Before each experimental trial, the reactor is heated to 250°C with inert flow. This heat input is maintained after the introduction of the reactants and for the duration of the experimental trial. The net reaction is exothermic, so reaction initiation produces an abrupt temperature rise in the reactor. After ∼1 h, the reactor reaches a steady state operating temperature. The reactor temperature ranges from 400 to 700°C, depending on the $i$C$_4$H$_{10}$ : O$_2$ ratio, total flow rate, and the catalyst. All data is collected at steady state, 1 h after reaction initiation. After each trial at a specific $i$C$_4$H$_{10}$ : O$_2$ ratio, the reaction is extinguished by replacing reactants with $N_2$ at the same flow rate. The flow of $O_2$ is removed first to prevent flammability. After the reactor cools, the process is repeated for a different $i$C$_4$H$_{10}$ : O$_2$ ratio.

In order to conduct experiments without $H_2$ removal, the lower copper gasket used to seal the membrane in the reactor module is replaced with a solid copper disk. The disk prevents any $H_2$ from being removed to the sweep side. The Pd foil is still present in these experiments, to account for any catalysis occurring on the Pd surface.

## 3. Results

### 3.1. Catalyst behavior in the absence of $H_2$ removal

In Fig. 6, typical conversions, selectivities, and reaction-side temperatures at various $i$C$_4$H$_{10}$ : O$_2$ ratios are reported for reaction over the Pt-monolith, Rh-monolith, and Pt-pellet catalysts. These data were acquired without $H_2$ separation at a total flow rate of 0.85 SLPM. Oxygen conversion is >98% for all experimental trials. Fig. 6a shows that both the autothermal reaction temperature and the isobutane conversion decrease as the $i$C$_4$H$_{10}$ : O$_2$ ratio increases away from the upper flammability limit ($i$C$_4$H$_{10}$ : O$_2$ ∼ 0.9). This behavior is typical of an exothermic oxidative dehydrogenation system operating with a constant heat input, and is observed for all three catalyst systems [35,36]. Fig. 6a also shows that the Pt pellets exhibit a reaction temperature higher than that of the other catalysts. This is due to increased $CO_2$ formation

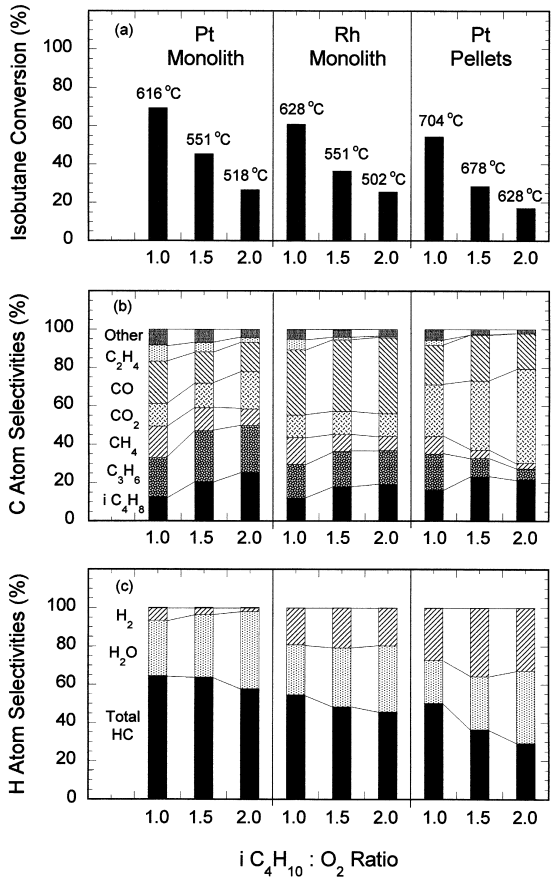


Fig. 6. (a) Isobutane conversion and reaction temperature, (b) C atom selectivities, and (c) H atom selectivities for Pt monolith, Rh monolith, and Pt pellets catalysts as a function of $i\mathrm{C_4H_{10}} : \mathrm{O_2}$ ratio at 0.85 SLPM for trials without $\mathrm{H_2}$ removal.

over the Pt-pellet catalyst, which causes the overall reaction to become more exothermic.

Fig. 6b,c show the selectivity for all carbon and hydrogen containing species. The Pt-monolith data confirm many of the trends observed previously for the oxidative dehydrogenation system [27]. At higher $i\mathrm{C_4H_{10}} : \mathrm{O_2}$ ratios, which correspond more closely to the stoichiometric ratio for oxidative dehydrogenation ($i\mathrm{C_4H_{10}} : \mathrm{O_2} = 2.0$), selectivity to isobutylene increases. At lower $i\mathrm{C_4H_{10}} : \mathrm{O_2}$ ratios, which approach the stoichiometric composition for syngas production ($i\mathrm{C_4H_{10}} : \mathrm{O_2} = 0.5$), selectivities to CO and $\mathrm{H_2}$ increase. In all cases, substantial cracking of $i\mathrm{C_4H_{10}}$ to $\mathrm{C_3H_6}$ and $\mathrm{CH_4}$ occurs.

Over the Rh monolith, there is a much higher selectivity to CO and $\mathrm{H_2}$ than over the Pt monolith for a given $i\mathrm{C_4H_{10}} : \mathrm{O_2}$ ratio. In addition, instead of decreasing with increasing $i\mathrm{C_4H_{10}} : \mathrm{O_2}$ ratio, selectivity to syngas remains fairly constant. These results are expected, since Rh is known to be an excellent catalyst for the production of syngas [26,36,37]. Cracking products ($\mathrm{C_3H_6}$, $\mathrm{C_2H_4}$, $\mathrm{CH_4}$) are still formed, but to a lesser extent than over Pt.

In the case of Pt pellets, selectivity to $\mathrm{CO_2}$ and $\mathrm{H_2}$ dominates. This difference can be attributed to the large surface area and more acidic nature of the $\gamma$-$\mathrm{Al_2O_3}$ present in the pellets, but absent in the $\alpha$-$\mathrm{Al_2O_3}$ monolith support. High surface area catalysts tend to be detrimental in catalytic systems where the desired product is a reactive intermediate [38]. In such systems, high surface area catalysts, particularly noble metals, favor complete combustion products.

### 3.2. Isobutylene yield improvement by $H_2$ removal

Fig. 7 shows the effect of $\mathrm{H_2}$ removal on isobutylene yield and reaction temperature at three $i\mathrm{C_4H_{10}} : \mathrm{O_2}$ ratios and two total flow rates over the Pt pellet catalyst and the 75 μm Pd membrane. At all $i\mathrm{C_4H_{10}} : \mathrm{O_2}$ ratios and total flow rates, $\mathrm{H_2}$ removal improves the isobutylene yield. This improvement is slightly greater at lower flow rates. Note that, with the reactor operated at a constant heat input, the removal of $\mathrm{H_2}$ is observed to lower the measured reaction temperature. Based on the thermodynamics in Fig. 2, a lower temperature should result in a lower $i\mathrm{C_4H_8}$ yield. Thus, the observed improvement in $i\mathrm{C_4H_8}$ yield with $\mathrm{H_2}$ removal is even more significant.

In Fig. 7, larger $i\mathrm{C_4H_8}$ yields occur at higher flows and lower $i\mathrm{C_4H_{10}} : \mathrm{O_2}$ ratios. These yields, however, are somewhat lower than those reported in previous studies [27]. Unfortunately, the design of this reactor leads to significant backmixing which reduces the achievable selectivity to reactive intermediate products ($i\mathrm{C_4H_8}$) in favor of final products (cracking products, CO, $\mathrm{CO_2}$). This is especially evident at the lower flow rates. However, this reactor design is convenient for the use of Pd foil as the membrane material. Foils are relatively simple to obtain, handle, and seal, making this a reasonable reactor design for screening experiments.

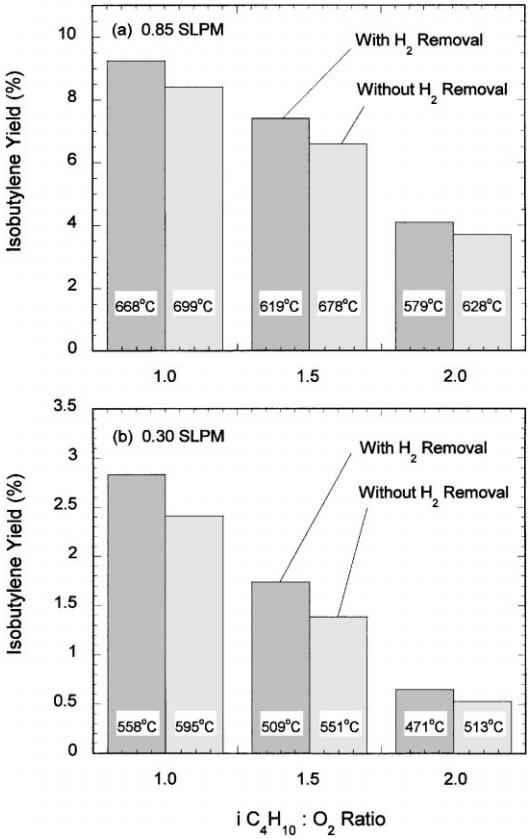


Fig. 7. Isobutylene yield and reaction temperature with and without $H_2$ removal through a 75-μm Pd membrane over Pt-pellet catalyst as a function of $iC_4H_{10}:O_2$ ratio at (a) 0.85 SLPM, and (b) 0.30 SLPM.

### 3.3. Effect of flow rate on $H_2$ removal

In Table 1, the partial pressure of $H_2$ in the sweep-side effluent is shown as a function of flow rate for the three catalysts investigated. The partial pressure of $H_2$ in the reaction side effluent is also shown. These experiments were conducted at a $iC_4H_{10}:O_2$ ratio of 1.0 with a 75-μm Pd membrane. As Table 1 shows, the partial pressure of $H_2$ on the sweep side was kept low at all times to maximize the transmembrane driving force.

If the total reaction-side flow rate is decreased from 0.85 to 0.30 SLPM for a *non-oxidative* dehydrogenation, one would expect that both, the reaction-side $H_2$ partial pressure and the permeation rate of $H_2$ would be unchanged. Since, in these experiments, the ratio of reaction and sweep-flow rates is kept constant, the partial pressure of $H_2$ on the sweep side would increase by a factor of ∼2.8 (or 0.85/0.30). The data recorded in Table 1 indicate that this is not at all what is observed in the oxidative dehydrogenation system. When the flow rate is decreased over the Pt pellets, the partial pressure of $H_2$ in the sweep effluent only increases by a factor of 1.2, while the $H_2$ partial pressure actually decreases over the Pt monolith. This behavior occurs because (unlike non-oxidative dehydrogenation), the partial pressure of $H_2$ driving permeation on the reaction side substantially decreases at the lower flow rate, as shown in Table 1. In this reaction system, the presence of $O_2$ causes an increase in the oxidation of $H_2$ to $H_2O$ at the lower flow rate. Therefore, as flow rate decreases (or catalyst contact time increases), the partial pressure of $H_2$ on the reaction side decreases, which counteracts the expected increase in the $H_2$ partial pressure in the sweep effluent. As a result of this behavior, the increase of catalyst contact time alone cannot substantially increase the impact of $H_2$ removal on the reaction system, as in non-oxidative dehydrogenation systems. Instead, it must be balanced to allow the Pd membrane enough time to remove a substantial fraction of the available $H_2$, yet not so long

Table 1
Effect of flow rate on partial pressure of $H_2$ in the sweep- and reaction-side effluents in trials with a 75-μm Pd membrane at an $iC_4H_{10}:O_2$ ratio of 1.0 over the Pt-monolith, Rh-monolith and Pt-pellet catalysts

| Catalyst | Flow (SLPM) | Catalyst contact time (s) | $H_2$ in sweep exit (Torr) | $H_2$ in reaction exit (Torr) |
|---|---|---|---|---|
| Pt pellets | 0.85 | 0.06 | 0.56 | 188.4 |
| | 0.30 | 0.25 | 0.69 | 63.7 |
| Pt monolith | 0.85 | 0.04 | 0.37 | 41.9 |
| | 0.30 | 0.16 | 0.18 | 5.03 |
| Rh monolith | 0.85 | 0.04 | 0.61 | 77.9 |
| | 0.30 | 0.16 | 1.25 | 72.9 |

Table 2
Effect of flow rate and Pd membrane thickness on the partial pressure of $H_2$ (Torr) in the sweep effluent at an $iC_4H_{10}:O_2$ ratio of 1.0 over the Pt-pellet catalyst

| Pd membrane thickness | Total flow rate | |
|---|---|---|
| | 0.30 SLPM | 0.85 SLPM |
| 75 μm | 0.69 | 0.56 |
| 25 μm | 1.99 | 0.73 |

a time that the available $H_2$ is completely oxidized to $H_2O$.

Although the partial pressure of $H_2$ in the reaction effluent decreases dramatically over the Pt catalysts at lower flow rates, Table 1 indicates that it only decreases slightly over the Rh monolith. This behavior can be attributed to the slow kinetics of $H_2O$ formation on Rh [37]. Consequently, the counteracting decrease in $H_2$ driving force occurs to a lesser extent, and the partial pressure of $H_2$ in the sweep effluent increases by a factor of 2.1, which is much closer to the 'expected' behavior.

### 3.4. Effect of membrane thickness on $H_2$ removal

Table 2 presents the effect that membrane thickness at two flow rates has on the partial pressure of $H_2$ in the sweep effluent. By decreasing the thickness of the Pd membrane from 75 to 25 μm at a constant flow rate, one would ideally expect to observe a factor of 3.0 increase in the sweep effluent $H_2$ partial pressure. For low flow rates, Table 2 indicates that the partial pressure of $H_2$ removed increases by a factor of 2.9, but at the higher flow rate, it only increases by a factor of 1.3. The diminished effect of membrane thickness at the higher flow rate is probably due to the combination of increased carbon deposition rates and higher temperatures. Such conditions can cause the rate limiting step of the transport process to shift from bulk diffusion to adsorption or absorption, thereby reducing the dependence on membrane thickness. This has been observed in other studies where poisonous species are present on the palladium surface [39,40]. There was no visual evidence to support other possibilities, such as the formation of palladium oxides or inadvertent incorporation of copper from the gasket into the Pd foil, both of which would result in a distinct color change in the metal.

## 4. Discussion

### 4.1. Necessary conditions for yield improvement by $H_2$ removal

Fig. 7 shows that removal of $H_2$ through a Pd membrane results in an isobutylene yield improvement for an oxidative dehydrogenation system. The extent of that improvement varies with flow rate, catalyst, and membrane thickness. In previous investigations of $H_2$-selective membrane reactors, it has been noted that the extent of yield improvement depends primarily on the balance of catalyst contact time and the time for $H_2$ removal across the membrane [13,14,18,23,41]. If the system is extremely diffusion limited (i.e. if the catalyst contact time is much shorter than the required time for $H_2$ removal across the membrane), $H_2$ removal has a limited impact on the product yield. This criterion can be summarized by the following characteristic time ratio:

$$\frac{\text{Catalyst contact time}}{\text{H}_2\text{ removal time}} = \frac{\tau_{\text{rxn}}}{\tau_{\text{rem}}} \equiv \frac{v_{\text{H}_2}}{v} = \frac{[P_{\text{m}}][p_{\text{H}_2}^{1/2}][A_{\text{m}}]}{[t_{\text{m}}][v]} \quad (5)$$

where $v_{H_2}$ is the volumetric flow of $H_2$ across the membrane, $v$ the total volumetric flow rate through the reaction side, $P_m$ the permeability coefficient of the membrane, $p_{H_2}$ the partial pressure of $H_2$ on the reaction side, $A_m$ the area of the membrane, and $t_m$ the thickness of the membrane. This expression assumes that the partial pressure of $H_2$ on the sweep side is negligible, which the data in Tables 1 and 2 support. The characteristic time ratio is experimentally determined using the ratio of volumetric flow rates, since both, $v$ and $v_{H_2}$ are measured quantities. This ratio is affected by several factors, as indicated in Eq. (5). As the value of the characteristic time ratio increases, the system becomes less diffusion limited, and $H_2$ removal results in greater improvements in isobutylene yield.

In the absence of $O_2$, the value of the characteristic time ratio can be increased simply by lowering the reaction side volumetric flow rate ($v$). However, for oxidative dehydrogenation over Pt catalysts, the partial pressure of $H_2$ on the reaction side ($p_{H_2}$) is strongly related to the reaction-side flow rate. A

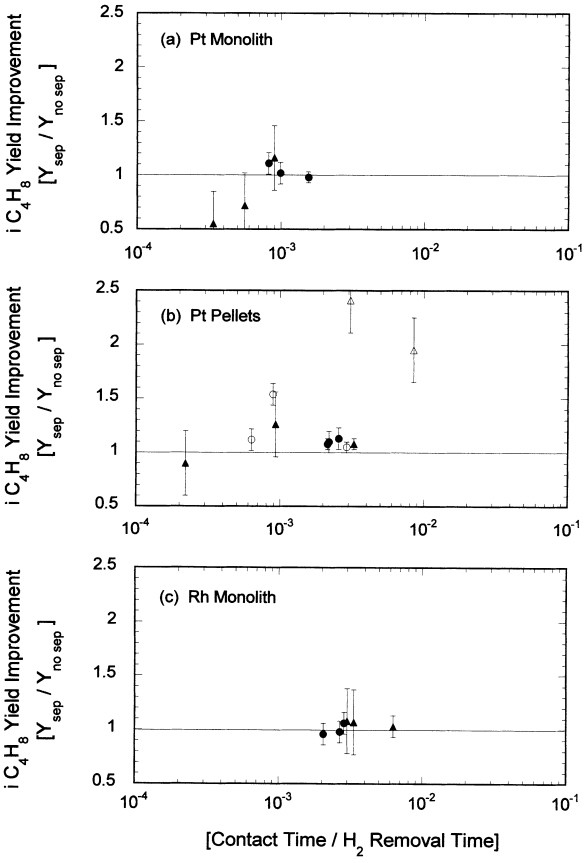


Fig. 8. Improvement in isobutylene yield as a function of the characteristic time ratio over (a) Pt-monolith, (b) Pt-pellet, and (c) Rh-monolith catalysts. Data represent experimental trials using the 75-μm Pd membrane at 0.85 and 0.30 SLPM (●, ▲, respectively) and trials using the 25 μm Pd membrane at 0.85 and 0.30 SLPM (○, △, respectively).

decrease in the flow rate affects the characteristic time ratio by decreasing both $v$ in the denominator and $p_{H_2}$ in the numerator of Eq. (5). Therefore, in oxidative dehydrogenation systems, the characteristic time ratio cannot be substantially increased (and may even decrease) with a decrease in total flow rate.

### 4.2. Yield improvement over various catalysts

In Fig. 8, isobutylene yield improvement (defined as the ratio of isobutylene yield with $H_2$ separation to the isobutylene yield without $H_2$ separation) is plotted against the ratio of catalyst contact time to $H_2$ removal time for the three different catalyst systems.

#### 4.2.1. Pt monolith

Fig. 8a presents the isobutylene yield improvement for the Pt monolith at various $i$C$_4$H$_{10}$ : O$_2$ ratios and total flow rates, using a 75-μm Pd membrane. In this case, the catalyst contact time is ∼1000 times shorter than the characteristic time for $H_2$ removal, so $H_2$ removal does not significantly improve isobutylene yield. A comparison of the high and low flow rate data in Fig. 8a indicates that decreasing the total flow rate actually can lower the ratio of catalyst contact time to $H_2$ removal time due to a decrease in $H_2$ partial pressure caused by oxidation to $H_2O$. Manipulation of the $i$C$_4$H$_{10}$ : O$_2$ ratio also influences the partial pressures of $H_2$ on the reaction side and affects the characteristic time ratio value, with the highest time-ratio values generally occurring at the lowest $i$C$_4$H$_{10}$ : O$_2$ ratios.

#### 4.2.2. Pt pellets

In Fig. 8b, an analogous plot is made for the Pt-pellet catalyst at different total flow rates, $i$C$_4$H$_{10}$ : O$_2$ ratios, and membrane thicknesses. This system is less membrane diffusion-limited than the Pt monolith, although catalyst contact time is still substantially less than the time for $H_2$ removal. The higher characteristic time ratios are primarily due to the increased production of $H_2$ in the Pt pellets. For the thinner membrane and the lower total flow data, the ratio approaches $10^{-2}$, and definite yield improvements can be observed. At lower ratio values, however, isobutylene yield is not improved by $H_2$ separation (i.e. a ratio of ∼1.0).

#### 4.2.3. Rh monolith

The Rh monolith data are shown in Fig. 8c. Higher selectivity to $H_2$ leads to characteristic time ratios approaching $10^{-2}$, similar to the Pt-pellet data. However, even at the highest ratio values, there is no indication of isobutylene yield improvement. This suggests that the dehydrogenation route in the Rh system is of little importance. The dominant route for $H_2$ production over Rh is partial oxidation to syngas. The isobutylene yield over Rh is not impeded by any equilibrium constraints imposed by dehydrogenation, and so the

removal of $H_2$ has only a limited effect on the reaction system. Fig. 8c also shows that, over this catalyst, decreasing the flow rate increases the characteristic time ratio as it would for a dehydrogenation in the absence of $O_2$. The loss of $H_2$ to $H_2O$ at lower flow rates does not readily occur over a Rh surface. Therefore, since $p_{H_2}$ is not a strong function of flow rate, the characteristic time ratio exhibits a more typical inverse relationship to the total flow rate.

## 5. Conclusions

We have considered the oxidative dehydrogenation of isobutane over Pt and Rh catalysts in a Pd membrane reactor. We have found that $H_2$ removal can improve isobutylene yield for cases where the ratio of catalyst contact time to $H_2$ removal time becomes large. Ideally, we would like this ratio to approach unity. However, due to the characteristic short catalyst contact times required for selective oxidation to $i C_4H_8$ over Pt catalysts, the system is most often extremely membrane diffusion-limited. Existing diffusion limitations cannot be overcome by a simple decrease in total flow rate, since this results in loss of $H_2$ to $H_2O$ (as well as a loss of $i C_4H_8$). To relieve the diffusion-limitations and achieve more substantial isobutylene yield improvements, reactor design variables must be manipulated. Thinner membranes with larger surface areas are an option, but there are practical limits to the adjustment of these variables. Efforts are underway to improve the reactor design to operate at lower total flow rates with less backmixing and more efficient membrane contacting.

We have also shown that, even with sufficient balance between catalyst contact time and $H_2$ removal time, yield improvements are only achieved in the presence of a good dehydrogenation catalyst, where the dehydrogenation route is actually imposing a substantial constraint on the isobutylene yield. In the oxidative dehydrogenation of isobutane over Rh, we found that no such constraint exists.

Although the yield improvements obtained in this study were modest, and the system may not currently be cost-effective, this work has helped to experimentally explore the boundaries of the region where Pd membranes can benefit a reaction system.

## References

[1] D. Seddon, Catal. Today 15 (1992) 1.
[2] R. Clark, R. Morris, D. Spence, E. Tucci, Energy Prog. 7 (1987) 164.
[3] T. Matsuda, I. Koike, N. Kubo, E. Kikuchi, Appl. Catal. A 96 (1993) 3.
[4] Z. Chen, A. Derking, W. Koot, M. Van Dijk, J. Catal. 161 (1996) 730.
[5] S. Udomask, R. Anthony, Ind. Eng. Chem. Res. 35 (1996) 47.
[6] S. Zdonik, in: L. Albright, B. Crynes, W. Corcoran (Eds.), Pyrolysis: Theory and Industrial Practice, Academic Press, New York, 1983, pp. 162, 392.
[7] M. Olbrich, D. McKay, D. Montgomery, US Patent 4926005 (Phillips Petroleum 1990).
[8] P. Van Diepen, et al., EP Patent 0561439 A2 (Shell Internationale Research Maatschappij B. V., 1993).
[9] B. Abdalla, S. Elnashaie, AIChE J. 40 (1994) 2055.
[10] J. Ali, D. Rippin, A. Baiker, Ind. Eng. Chem. Res. 34 (1995) 2940.
[11] J. Ali, A. Baiker, Appl. Catal. A 155 (1997) 41.
[12] J. Collins, et al., Ind. Eng. Chem. Res. 35 (1996) 4398.
[13] J. Deng, J. Wu, Appl. Catal. A 109 (1994) 63.
[14] J. Deng, Z. Cao, B. Zhou, Appl. Catal. A 132 (1995) 9.
[15] E. Gobina, R. Hughes, J. Membr. Sci. 90 (1994) 11.
[16] E. Gobina, R. Hughes, Chem. Eng. Sci. 51 (1996) 3045.
[17] E. Gobina, R. Hughes, Appl. Catal. A 137 (1996) 119.
[18] T. Ioannides, G. Gavalas, J. Membr. Sci. 77 (1993) 207.
[19] N. Itoh, W. Xu, K. Haraya, J. Membr. Sci. 66 (1992) 149.
[20] T. Kikuchi, Catal. Today 25 (1995) 333.
[21] Y. Cao, B. Liu, J. Deng, Appl. Catal. A 154 (1997) 129.
[22] J. Shu, et al., Can. J. Chem. Eng. 75 (1997) 712.
[23] H. Weyten, K. Keizer, A. Kinoo, J. Luyten, R. Leysen, AIChE J. 43 (1997) 1819.
[24] V. Zaspalis, et al., Appl. Catal. 74 (1991) 223.
[25] B. Raich, H. Foley, Appl. Catal. A 129 (1995) 167.
[26] S. Bharadwaj, L. Schmidt, J. Catal. 155 (1995) 403.
[27] M. Huff, L. Schmidt, J. Catal. 155 (1995) 82.
[28] HYSYS NetVers. v 1.2.2, Hyprotech Ltd., Calgary, 1997.
[29] E. Wicke, H. Brodowsky, in: G. Alefeld, J. Volkl (Eds.), Hydrogen in Metals, vol. 2, Springer, New York, 1978, p. 73.
[30] Y. Balovnev, Russ. J. Phys. Chem. 48 (1974) 409.
[31] S. Koffler, J. Hudson, G. Ansell, Trans. AIME 245 (1969) 1735.
[32] V. Pugachev, F. Busol, E. Nikolaev, B. Nam, Russ. J. Phys. Chem. 49 (1975) 1045.
[33] L. Rubin, Englehard Ind. Tech. Bull. 7 (1966) 55.
[34] D. Flick, M. Huff, J. Catal. 178 (1998) 315.
[35] T. Raybold, M. Huff, Stud. Surf. Sci. Catal. 110 (1997) 501.
[36] M. Huff, L. Schmidt, J. Phys. Chem. 97 (1993) 11815.
[37] D. Hickman, L. Schmidt, Science 259 (1993) 343.
[38] B. Gates, Catalytic Chemistry, Wiley, New York, 1992, 236 pp.
[39] C. Peden, B. Kay, D. Goodman, Surf. Sci. 175 (1986) 215.
[40] F. Chen, Y. Kinari, F. Sakamoto, Y. Nakayama, Y. Sakamoto, Int. J. Hydrogen Energy 21 (1996) 551.
[41] T. Ioannides, X. Verykios, Catal. Lett. 36 (1996) 165.